

THROMBOSIS AND HEMOSTASIS

Cytoprotective activated protein C averts Nlrp3 inflammasome–induced ischemia-reperfusion injury via mTORC1 inhibition

Sumra Nazir,¹ Ihsan Gadi,¹ Moh'd Mohanad Al-Dabet,¹ Ahmed Elwakiel,¹ Shrey Kohli,¹ Sanchita Ghosh,¹ Jayakumar Manoharan,¹ Satish Ranjan,¹ Fabian Bock,^{1,2} Ruediger C. Braun-Dullaeus,³ Charles T. Esmon,^{4,5} Tobias B. Huber,⁶ Eric Camerer,⁷ Chris Dockendorff,⁸ John H. Griffin,⁹ Berend Isermann,^{1,*} and Khurram Shahzad^{1,10,*}

¹Department of Clinical Chemistry and Pathobiochemistry, Otto-von-Guericke-University, Magdeburg, Germany; ²Department of Medicine, Vanderbilt University Medical Center, Nashville, TN; ³Division of Cardiology and Angiology, Department of Internal Medicine, Otto-von-Guericke-University, Magdeburg, Germany; ⁴Coagulation Biology Laboratory, Oklahoma Medical Research Foundation, Oklahoma City, OK; ⁵Departments of Pathology and Biochemistry and Molecular Biology, University of Oklahoma Health Sciences Center, Oklahoma City, OK; ⁶Department of Medicine III, University Medical Center Hamburg-Eppendorf, Hamburg, Germany; ⁷INSERM U970, Paris Cardiovascular Research Centre, Paris, France; ⁸Department of Chemistry, Marquette University, Milwaukee, WI; ⁹Department of Molecular Medicine, The Scripps Research Institute, La Jolla, CA; and ¹⁰Department of Biotechnology, University of Sargodha, Sargodha, Pakistan

Key Points

- aPC protects from myocardial and renal IRIs by restricting mTORC1-mediated activation of the Nlrp3 inflammasome.
- Nlrp3 inflammasome suppression by aPC is independent of its anticoagulant effect, depends on PAR-1, and can be mimicked by parmodulin-2.

Cytoprotection by activated protein C (aPC) after ischemia-reperfusion injury (IRI) is associated with apoptosis inhibition. However, IRI is hallmarked by inflammation, and hence, cell-death forms disjunct from immunologically silent apoptosis are, in theory, more likely to be relevant. Because pyroptosis (ie, cell death resulting from inflammasome activation) is typically observed in IRI, we speculated that aPC ameliorates IRI by inhibiting inflammasome activation. Here we analyzed the impact of aPC on inflammasome activity in myocardial and renal IRIs. aPC treatment before or after myocardial IRI reduced infarct size and Nlrp3 inflammasome activation in mice. Kinetic in vivo analyses revealed that Nlrp3 inflammasome activation preceded myocardial injury and apoptosis, corroborating a pathogenic role of the Nlrp3 inflammasome. The constitutively active *Nlrp3*^{A350V} mutation abolished the protective effect of aPC, demonstrating that Nlrp3 suppression is required for aPC-mediated protection from IRI. In vitro aPC inhibited inflammasome activation in macrophages, cardiomyocytes, and cardiac fibroblasts via proteinase-activated receptor 1 (PAR-1) and mammalian target of rapamycin complex 1

(mTORC1) signaling. Accordingly, inhibiting PAR-1 signaling, but not the anticoagulant properties of aPC, abolished the ability of aPC to restrict Nlrp3 inflammasome activity and tissue damage in myocardial IRI. Targeting biased PAR-1 signaling via parmodulin-2 restricted mTORC1 and Nlrp3 inflammasome activation and limited myocardial IRI as efficiently as aPC. The relevance of aPC-mediated Nlrp3 inflammasome suppression after IRI was corroborated in renal IRI, where the tissue protective effect of aPC was likewise dependent on Nlrp3 inflammasome suppression. These studies reveal that aPC protects from IRI by restricting mTORC1-dependent inflammasome activation and that mimicking biased aPC PAR-1 signaling using parmodulins may be a feasible therapeutic approach to combat IRI. (*Blood*. 2017;130(24):2664-2677)

Introduction

Myocardial infarction (MI) is a major cause of death worldwide. Rapid diagnosis and reperfusion improve survival after MI. However, cardiac ischemia-reperfusion injury (IRI) triggers pronounced tissue-disruptive and sterile proinflammatory responses, which compromise outcome.¹⁻³ Induction of interleukin-1 β (IL-1 β) and IL-18, which are controlled by the Nlrp3 inflammasome, contribute to the tissue-disruptive and proinflammatory responses.^{4,5} Importantly, Nlrp3 inflammasome inhibition reduces infarct size, attenuates adverse cardiac remodeling, and preserves cardiac function in animal models of MI.⁶⁻⁸

The inflammasome is a signaling platform detecting pathogenic microorganisms and sterile stressors.⁹ Sensor molecules, which typically

contain a NOD-like receptor (Nlr; eg, Nlrp1, Nlrp3, or Nlrp4), detect appropriate stimuli and form a complex with ASC, an adaptor protein encoded by PYCARD. ASC contains a pyrin domain and a caspase activation and recruitment domain (CARD). Via its pyrin domain, ASC interacts with the sensor molecule, and the CARD domain interacts with caspase-1 and initiates caspase-1 self-cleavage. Activated caspase-1 proteolytically activates pro-IL-1 β and pro-IL-18, inducing their release via a nonclassical secretion pathway. The activation of the Nlrp3 inflammasome comprises 2 steps: during the priming step, Nlrp3 expression is induced, and during the activation step, the oligomeric inflammasome complex assembles, inducing maturation of IL-1 β and IL-18.⁹

Submitted 1 May 2017; accepted 1 September 2017. Prepublished online as *Blood* First Edition paper, 7 September 2017; DOI 10.1182/blood-2017-05-782102.

*B.I. and K.S. contributed equally as last authors.

The online version of this article contains a data supplement.

There is an Inside *Blood* Commentary on this article in this issue.

The publication costs of this article were defrayed in part by page charge payment. Therefore, and solely to indicate this fact, this article is hereby marked "advertisement" in accordance with 18 USC section 1734.

© 2017 by The American Society of Hematology

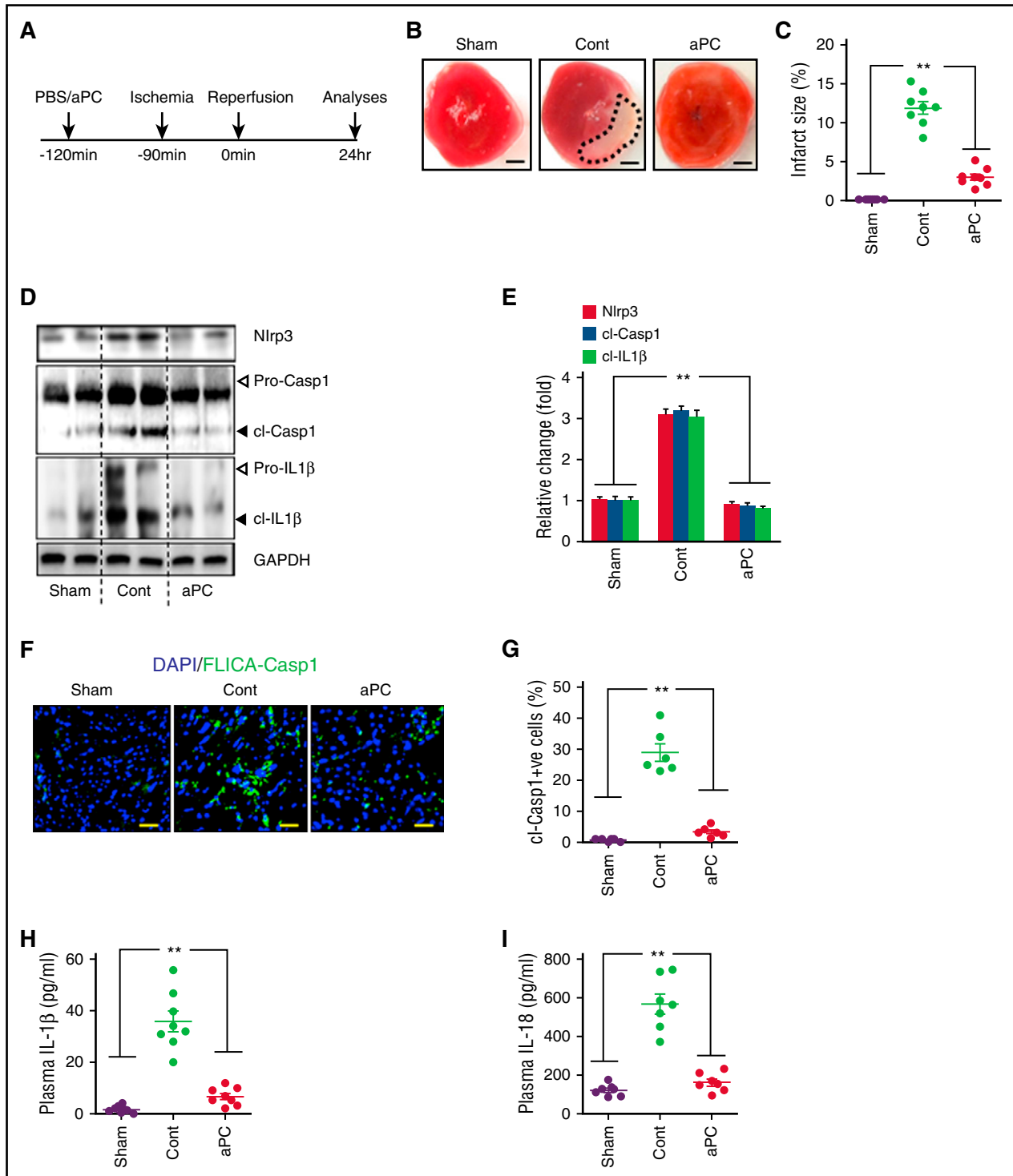


Figure 1. aPC ameliorates inflammasome activation after myocardial IRI. (A) Experimental design. (B-C) aPC treatment reduces infarct size. Representative heart sections showing infarcted area detected by triphenyl tetrazolium chloride staining (area encircled by dashed line; size bar, 20 μ m) (B) and dot plot summarizing data (C). (D-I) aPC pretreatment significantly reduces cardiac Nlrp3 expression and cleavage of caspase-1 (cl-Casp1) and IL-1 β (cl-IL-1 β). Representative immunoblots (glyceraldehyde-3-phosphate dehydrogenase [GAPDH]; loading control [cont]) (D) and bar graph summarizing data (E). Arrowheads indicate inactive (white) and active (black) forms of caspase-1 or IL-1 β (D). The active form was quantified (E). aPC treatment reduces caspase-1 activity within infarcted area. Representative images of frozen sections incubated with FLICA-Casp1 probes (size bar, 20 μ m) (F) and dot plot summarizing data (G). aPC reduces plasma IL-1 β (H) and IL-18 levels (I) after myocardial IRI; dot plots summarizing data. Sham-operated mice (sham) or mice with myocardial IRI without (cont; PBS) or with aPC pretreatment (aPC). Data shown represent mean \pm SEM of at least 6 mice per group. * P < .05, ** P < .01; analysis of variance (C,E,H,I) or Mann-Whitney U test (G).

IL-1 receptor antagonist is an endogenous Nlrp3 inflammasome inhibitor during IRI.^{10,11} However, its induction after myocardial IRI is insufficient to provide full protection, which may reflect higher

affinity of IL-1 for the receptor or excess availability of IL-1 receptor.¹² Thus, deciphering independent pathways enabling Nlrp3 inflammasome restriction is required to identify suitable therapeutic

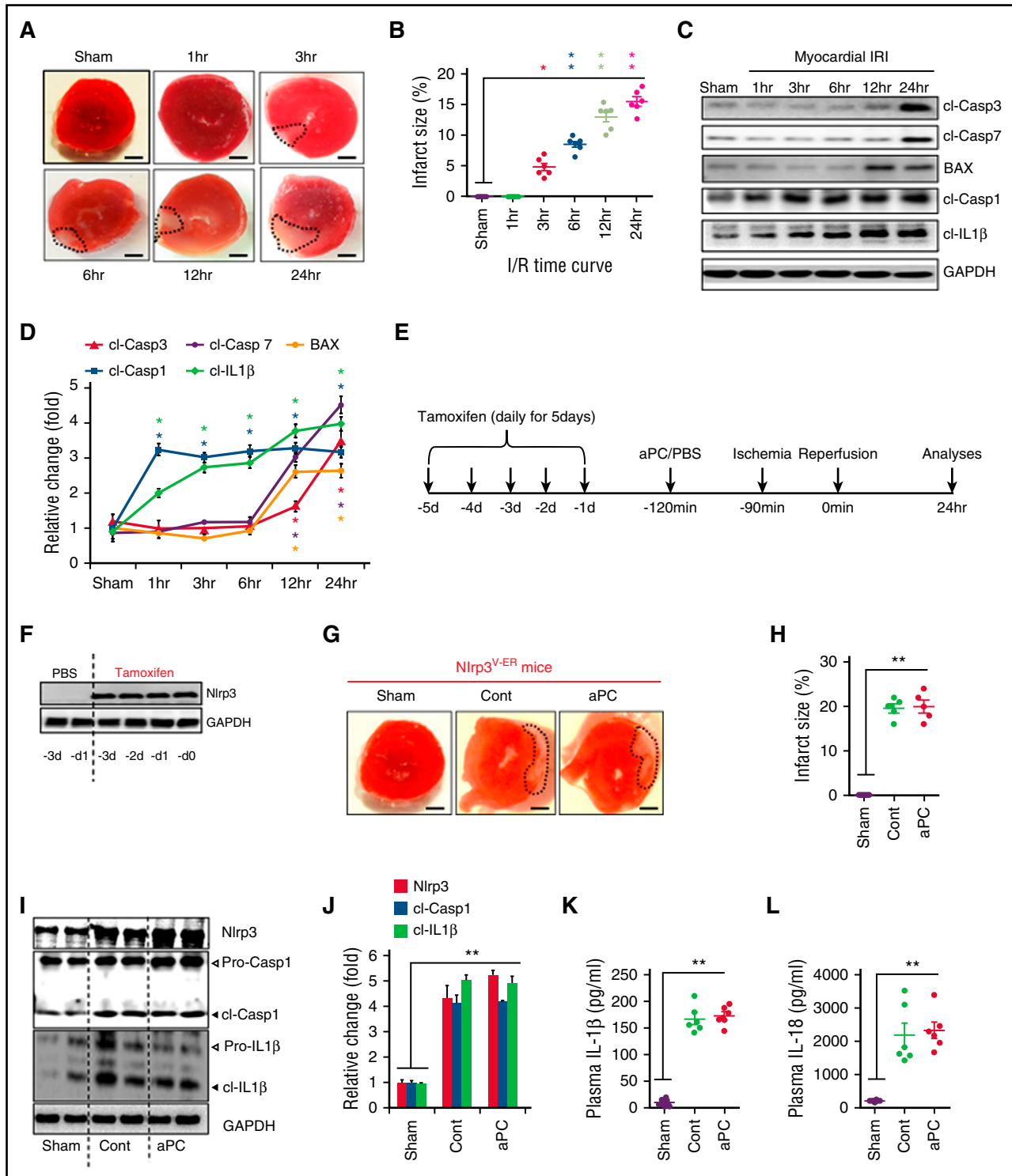
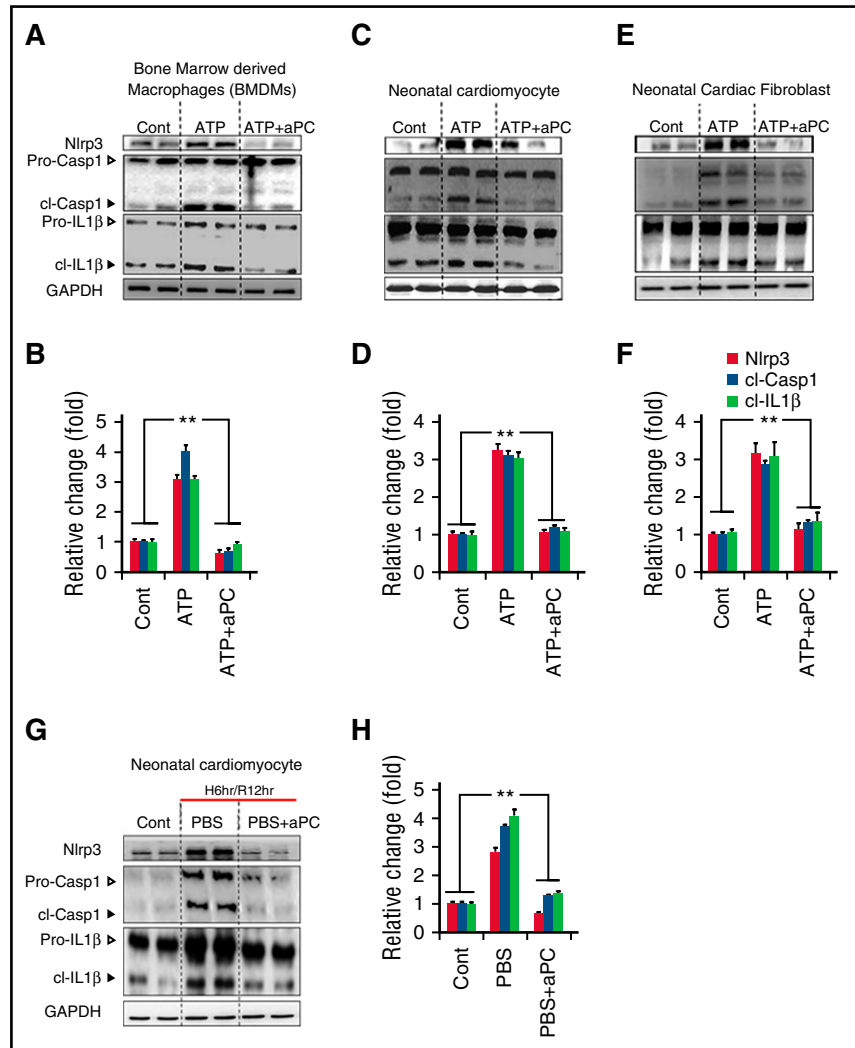


Figure 2. Pivotal function of Nlrp3 inflammasome in myocardial IRI. (A-D) Kinetic analyses of infarct size and markers of inflammasome and apoptosis activation in hearts isolated at various time points after IRI (1-24 hours) compared with sham-operated mice. Representative images of triphenyl tetrazolium chloride (TTC) staining (infarct area encircled by dashed line; size bar, 20 μ m) (A), dot plot summarizing data of infarct size (individual data points and mean \pm SEM) (B), and representative immunoblots of inflammasome (cl-Casp1, cl-IL-1 β) or apoptosis activation (cl-Casp3, cl-Casp7, BAX expression) markers, with glyceraldehyde-3-phosphate dehydrogenase [GAPDH] as loading control (C). (D) Line graph summarizing immunoblot data (mean \pm SEM). (E) Experimental design. (F-H) Constitutively active Nlrp3^{A350V} abolishes the protective effect of aPC in myocardial IRI. (F) Induction of Nlrp3^{A350V} expression after tamoxifen injection into Nlrp3^{A350V} mice compared with PBS-treated mice; representative immunoblots, with GAPDH as loading control. (G-H) aPC treatment fails to protect against myocardial IRI in Nlrp3^{V-ER} mice. Representative heart sections showing infarcted area detected by TTC staining (area encircled by dashed line; size bar, 20 μ m) (G) and dot plot summarizing data (H). (I-L) aPC fails to reduce Nlrp3 expression, cl-Casp1 or cl-IL-1 β , or plasma IL-1 β and IL-18 levels in Nlrp3^{V-ER} mice after myocardial IRI. Representative immunoblots (I) and bar graphs (J) summarizing results, with GAPDH as loading control; arrowheads indicate inactive (white) and active (black) forms of caspase-1 or IL-1 β (I). (J) The active form was quantified. (K-L) Dot plots of plasma IL-1 β and IL-18 levels. Sham-operated mice (sham) or mice with myocardial IRI without (cont; PBS) or with aPC pretreatment (aPC). Data shown represent mean \pm SEM of at least 6 mice per group. * P < .05, ** P < .01; Student t test (B,D) or analysis of variance (H,J,L).

Figure 3. aPC prevents inflammasome activation in cardiac resident cells and macrophages in vitro. (A-F) In mouse BMDMs (A-B), mouse neonatal cardiomyocytes (C-D), and mouse neonatal cardiac fibroblasts (E-F), inflammasome activation was induced by priming with LPS (500 ng/mL, 3 hours) followed by ATP (10 μ M, 3 hours; control [cont]: PBS). Concomitant treatment with aPC (20 nM; added once 30 minutes before ATP stimulation) markedly reduced the LPS/ATP-mediated induction of Nlrp3 and cl-Casp1 and cl-IL-1 β ; representative immunoblots (A,C,E) and corresponding bar graphs summarizing results (B,D,F). Arrowheads indicate inactive (white) and active (black) forms of caspase-1 or IL-1 β (A,C,E). (B,D,F) The active form was quantified. (G-H) Nlrp3 expression and cl-Casp1 and cl-IL-1 β are increased in mouse neonatal cardiomyocytes subjected to 6 hours of hypoxia (H; 1% oxygen) and serum and glucose deprivation (Hanks balanced salt solution medium), followed by 12 hours of reoxygenation (R; 21% oxygen) in complete medium. H/R induces inflammasome activation, which is prevented by aPC (20 nM; added once at the time of R); representative immunoblots of whole-cell lysates (G) and bar graph summarizing results (H), with glyceraldehyde-3-phosphate dehydrogenase (GAPDH) as loading control. (G) Arrowheads indicate inactive (white) and active (black) forms of caspase-1 or IL-1 β , respectively. (H) The active form was quantified. Data shown represent mean \pm SEM. Data obtained from at least 3 independent experiments, each with at least 2 technical replicates (A-H); GAPDH as loading control (A,C,E,G). ** $P < .01$; analysis of variance (B,D,F,H).



strategies. Like inflammation, mammalian target of rapamycin (mTOR) signaling and coagulation proteases modulate myocardial IRI, but whether these systems are mechanistically linked remains unknown.^{13,14}

An important endogenous inhibitor of inflammation is the coagulation protease-activated protein C (aPC). Given its strong anti-inflammatory properties, human recombinant aPC received approval for sepsis treatment, but it was eventually withdrawn from the market, partially because of failure to replicate efficacy.^{15,16} Variants of aPC with reduced anticoagulant activity are currently undergoing clinical evaluation for stroke¹⁵ (registered at www.clinicaltrials.gov as #NCT02222714). In regard to myocardial IRI, several studies have demonstrated cardioprotection by aPC, which has been linked with apoptosis inhibition.¹⁷⁻²² However, apoptosis is an immunogenically silent cell-death form and is less likely to promote myocardial IRI than other cell-death forms associated with inflammation, such as pyroptosis.²³ Considering the close association of myocardial IRI, as well as other forms of IRI, with a strong sterile inflammatory response and the anti-inflammatory effect of aPC, we hypothesized that aPC restricts inflammasome activation in IRI.

Methods

See the supplemental Data, available on the *Blood* Web site, for additional information.

Mice

Proteinase-activated receptor 2^{-/-} (PAR-2^{-/-}), (PAR-3^{-/-}), Nlrp3^{A350V LoxP/LoxP}, and RosaERT^{Cre} mice were obtained from Jackson Laboratory (Bar Harbor, ME). PAR-1^{-/-} and TSC1^{LoxP/LoxP} mice were kindly provided by E.C. (Paris, France) and T.B.H. (Hamburg, Germany), respectively. Wild-type mice (C57BL/6) were obtained from Janvier Labs (Le Genest-Saint-Isle, France). In the current study, we used littermates that had been backcrossed for at least 10 generations on a C57BL/6J background. Only age-matched mice were used throughout the study. All animal experiments were conducted following standards and procedures approved by the local animal care and use committee (Landesverwaltungsamt, Halle, Germany).

In vivo intervention studies

For the myocardial IRI model (left anterior descending artery ligation for 90 minutes followed by 24 hours of reperfusion), mice were injected with phosphate-buffered saline (PBS; control; equal volume intraperitoneally [IP]), aPC (1 mg/kg IP),²⁴ aPC-HAPC1573 complex (aPC was preincubated before injection with HAPC1573 antibody at a 1:1 molar ratio for 10 minutes under gentle agitation to block its anticoagulant activity),²⁴⁻²⁷ an aPC variant lacking specifically anticoagulant function (3K3A-aPC; 1 mg/kg IP),^{28,29} the inhibitory PAR-1 pepducin (P1pal-12S; 2.5 mg/kg subcutaneously) followed by aPC (1 mg/kg IP),^{26,30,31} or parmodulin-2 (5 mg/kg IV)³² 30 minutes before myocardial IRI. A subset of mice was treated with PBS (control; equal volume IP) or aPC (1 mg/kg IP) 30 minutes after starting reperfusion. In renal IRI experiments (bilateral renal pedicle occlusion for 30 minutes followed by 24 hours of

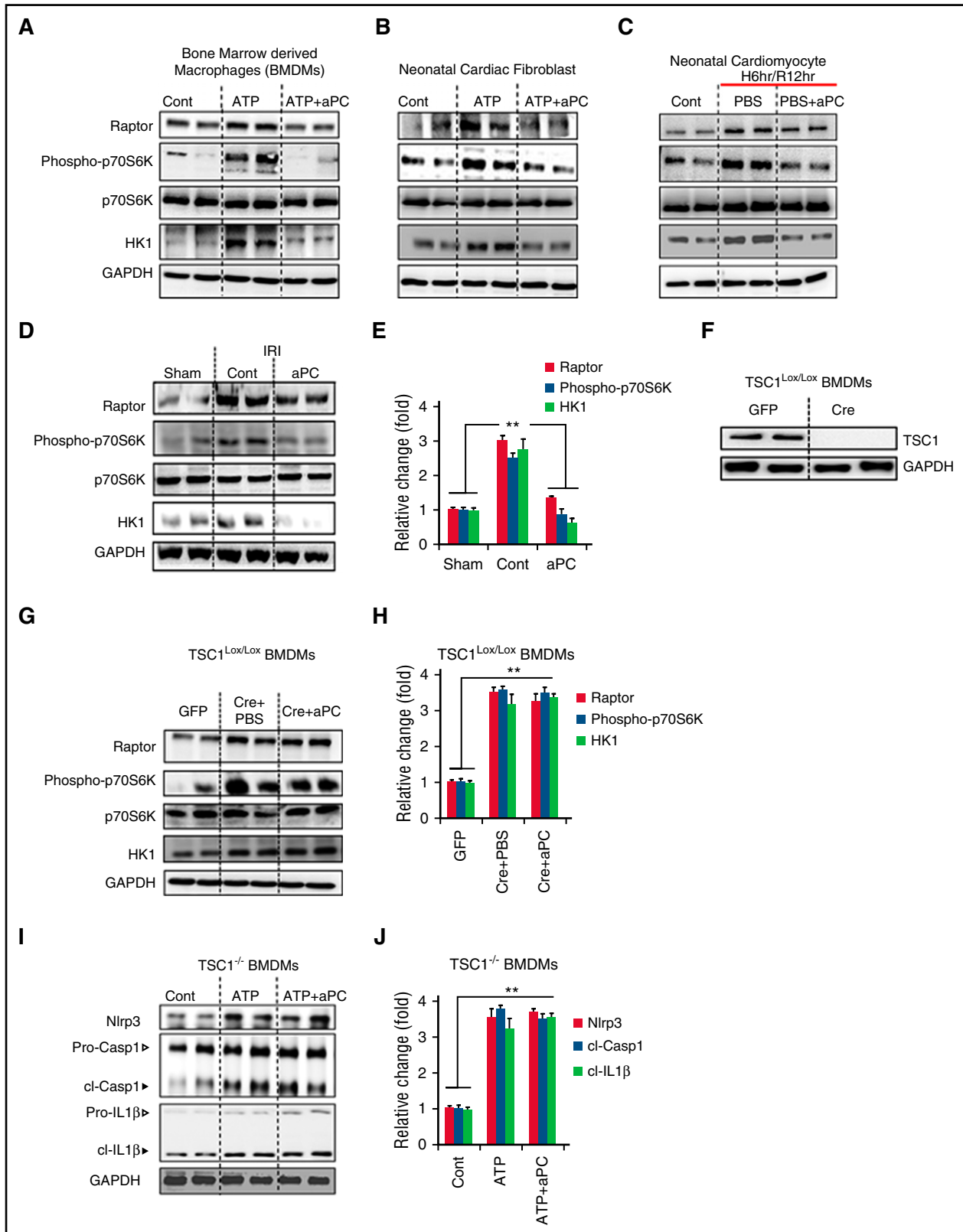


Figure 4. aPC restricts inflammasome by suppressing mTORC1. (A-C) Expression of Raptor, and HK1 and phosphorylation (phospho) of ribosomal p70-S6 kinase (pS6K70) were analyzed in LPS-primed and ATP-challenged BMDMs (A) and mouse neonatal cardiac fibroblasts (B) or mouse neonatal cardiomyocytes subjected to hypoxia/reoxygenation (H/R) (C). aPC inhibits expression of Raptor and HK1 and p70S6K phosphorylation levels in LPS-primed and ATP-stimulated cells (A-B) or in H/R-injured primary cardiomyocytes (C). (D-E) Treatment of mice with aPC inhibits mTORC1 signaling; representative immunoblots showing cardiac Raptor and HK1 expression as well as total and phosphorylated pS6K70. Representative immunoblots (D) and bar graph summarizing results (E). (F-J) BMDMs from TSC1^{LoxP/LoxP} mice were transiently transfected with GFP- or Cre-expressing plasmids, resulting in loss of TSC1 expression after 48 hours. Representative immunoblots of TSC1, with glyceraldehyde-3-phosphate dehydrogenase (GAPDH) as loading control (cont) (F). (G-H) In TSC1-deficient BMDM cells, aPC treatment fails to reduce Raptor or HK1 expression or

reperfusion),²⁵ mice were injected with PBS (control; 1 mg/kg IP) or aPC (1 mg/kg IP) 30 minutes before IRI. P1pal-12S and parrmodulin-2 have been previously described.³⁰⁻³³ Infarct size was determined as described in the supplemental Methods.

Caspase-1 activity assay

Caspase-1 activity was determined on frozen heart sections using the FLICA Casp-1 assay (Immunochemistry Technologies LCC) as described.³⁴

Cell culture

Primary mouse bone marrow–derived macrophages (BMDMs), neonatal cardiomyocytes, and neonatal cardiac fibroblasts were isolated and cultured as described elsewhere.^{35,36}

Statistical analysis

The data are summarized as the mean \pm standard error of the mean (SEM). Statistical analyses were performed with the Student *t* test, the Mann-Whitney *U* test, or analysis of variance, as appropriate. Post hoc comparisons of analysis of variance were corrected with the method of Tukey. The Kolmogorov-Smirnov test or the D'Agostino-Pearson normality test was used to determine whether the data were consistent with a Gaussian distribution. Prism 5 software (www.graphpad.com) was used for statistical analyses. Statistical significance was accepted at *P* values $< .05$.

Results

aPC restricts inflammasome activation after myocardial IRI

To determine whether aPC restricts inflammasome activation in myocardial IRI, we treated mice with aPC (1 mg/kg IP) or PBS (control). After 30 minutes, we induced myocardial ischemia for 90 minutes and analyzed mice after 24 hours of reperfusion (Figure 1A). Congruent with previous reports, aPC markedly reduced infarct size (Figure 1B-C).¹⁷⁻²² Reduction of infarct size by aPC was associated with reduced inflammasome activation within the heart. Cardiac expression of Nlrp3 and cl-Casp1 and cl-IL-1 β were increased after myocardial IRI but reduced after aPC pretreatment (Figure 1D-E). Concurrently, in situ caspase-1 activity after myocardial IRI was reduced by aPC (Figure 1F-G). These changes were reflected by plasma cytokine levels. Thus, increased plasma IL-1 β and IL-18 levels after myocardial IRI were attenuated by aPC (Figure 1H-I). Additionally, treatment with aPC after myocardial IRI reduced myocardial infarct size and markers of inflammasome activation within the heart and plasma as efficiently as aPC pretreatment (supplemental Figure 1A-G). Thus, aPC efficiently restricts inflammasome activation after myocardial IRI.

Inflammasome activation precedes apoptosis after myocardial IRI

Amelioration of myocardial IRI by aPC has been associated with reduced apoptosis, an immunologically silent form of cell death. However, myocardial IRI is strongly associated with inflammation,³⁷ and hence, we speculated that inflammasome activation might be the leading pathomechanism. To gain insights into the temporal pattern of

inflammasome and apoptosis activation after myocardial IRI, we conducted kinetic studies. Hearts isolated at various time points after reperfusion (1-24 hours) were compared with hearts of sham-operated mice. An infarcted area was detected as early as 3 hours after reperfusion (Figure 2A-B). Inflammasome activation within the heart preceded the detectable infarcted area (1-hour time point; cl-Casp1 and cl-IL-1 β ; Figure 2C-D), whereas markers of apoptosis activation increased at later time points (12-hour time point; cl-Casp3, cl-Casp7, BAX; Figure 2C-D). These data establish that myocardial inflammasome activation occurs early in IRI and precedes the detection of an infarcted area and, importantly, apoptosis activation.

Constitutively active Nlrp3 abolishes the protective effect of aPC in myocardial IRI

The kinetics of inflammasome and apoptosis activation after myocardial IRI suggest that inflammasome activation is the culprit and hence that inflammasome suppression is the primary mechanism underlying the cytoprotective effect of aPC after myocardial IRI. To ascertain whether inflammasome restriction is required for the protective effect of aPC in myocardial IRI, we crossed mice containing an inducible Nlrp3 gain-of-function mutation (Nlrp3^{A350V} LoxP/LoxP [LoxP-Cre recombinase–dependent expression of the constitutively active Nlrp3^{A350V} mutation]) with mice ubiquitously expressing inducible Cre recombinase under the control of the estrogen receptor T2 (Rosa Cre-ER^{T2}), yielding Nlrp3^{A350V} LoxP/LoxP \times Rosa Cre-ER^{T2} mice (hereafter referred to as Nlrp3^{V-ER} mice). Expression of the Nlrp3^{A350V} mutation does not cause heart injury by itself and requires a second stimulus for inflammasome activation.³⁸ Mice were treated for 5 days with tamoxifen (5 mg/kg IP) or PBS (control), which increased Nlrp3 expression in tamoxifen-treated mice (Figure 2E-F). Mice were injected with aPC or PBS (control) 24 hours after the last tamoxifen injection. After another 30 minutes, myocardial ischemia was induced for 90 minutes, and analyses were conducted 24 hours after reperfusion (Figure 2E). In tamoxifen-treated but sham-operated mice, no myocardial infarction was detected (Figure 2G-H), and indices of inflammasome activation remained normal (Figure 2I-L), corroborating that expression of Nlrp3^{A350V} mutation is not sufficient to cause myocardial inflammasome activation. After myocardial IRI, an infarcted area was readily detectable in Nlrp3^{V-ER} mice (Figure 2G-H). Importantly, aPC treatment failed to reduce the infarct size in Nlrp3^{V-ER} mice (Figure 2G-H). Concurrently, aPC failed to reduce protein levels of Nlrp3, cl-Casp1 or cl-IL-1 β (Figure 2I-J), or plasma IL-1 β and IL-18 levels (Figure 2K-L) in Nlrp3^{V-ER} mice after myocardial IRI. These data establish that in mice with a genetically superimposed bias for inflammasome activation, the protective effect of aPC in myocardial IRI is lost.

aPC prevents inflammasome activation in cardiac resident cells and macrophages in vitro

The role of the inflammasome in innate immune cells like macrophages is firmly established, but recent data have demonstrated functional inflammasome in tissue-resident cells, including cardiomyocytes.^{6,8} To identify in which cell types aPC prevents inflammasome activation

Figure 4 (continued) phosphorylation of p70S6K (TSC1^{LoxP/LoxP}+Cre+aPC) when compared with PBS-treated cells (TSC1^{LoxP/LoxP}+Cre+PBS) Representative immunoblots (G) and bar graph summarizing results (H). (I-J) Likewise, aPC fails to reduce Nlrp3 expression or cl-Casp1 or cl-IL-1 β in TSC1-deficient BMDMs. Representative immunoblots (I) and bar graph summarizing results (J). (I) Arrowheads indicate inactive (white) and active (black) forms of caspase-1 or IL-1 β . (J) The active form was quantified. Data shown represent mean \pm SEM. Data obtained from at least 3 independent experiments each with at least 2 technical replicates (A-J); GAPDH as loading control (A-D,F-G,I). ***P* $< .01$; analysis of variance (E,H,J).

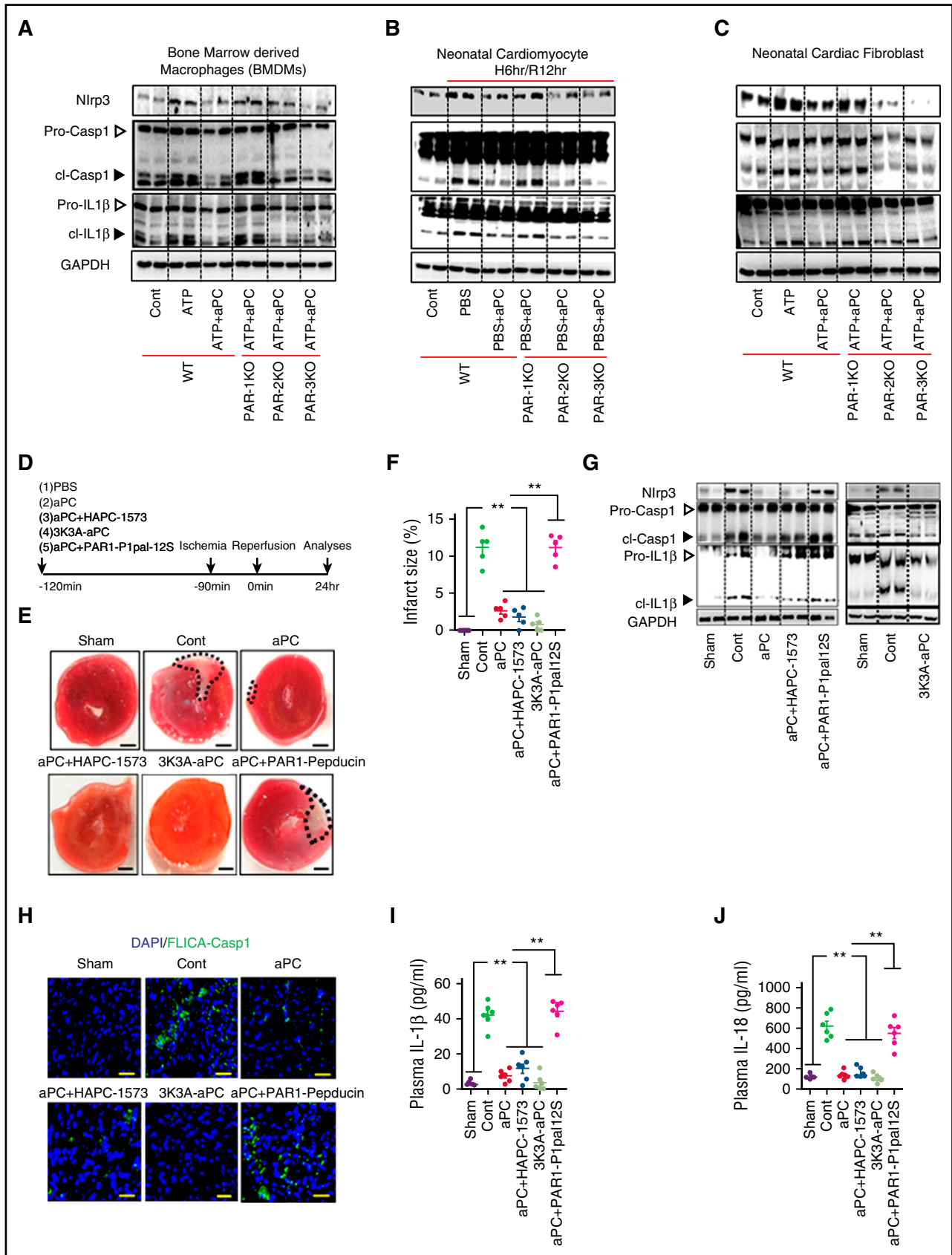


Figure 5. aPC restricts inflammasome activation via PAR-1 after myocardial IRI. (A-C) The effect of aPC on inflammasome activation was analyzed after receptor inhibition. BMDMs (A), neonatal cardiomyocytes (B), or neonatal cardiac fibroblasts (C) were isolated from wild-type (WT), PAR-1^{-/-}, PAR-2^{-/-}, or PAR-3^{-/-} mice. aPC fails to suppress LPS/ATP- (A,C) or hypoxia/reoxygenation-induced (B) Nlrp3 expression and cl-Casp1 and cl-IL-1β in the absence of PAR-1 in all cell types, whereas loss of other receptors had no effect; representative immunoblots, with glyceraldehyde-3-phosphate dehydrogenase (GAPDH) as loading control (A-C). (D) Experimental design.

in myocardial IRI, we isolated primary BMDMs, primary neonatal cardiomyocytes, and primary neonatal cardiac fibroblasts. Cells were primed with lipopolysaccharide (LPS; 500 ng/mL), and after 3 hours, cells were exposed to aPC (20 nM) or PBS (control). After 1 hour, cells were exposed to adenosine triphosphate (ATP) or PBS (control) for 3 hours to activate the Nlrp3 inflammasome.^{39,40} The LPS/ATP-mediated induction of Nlrp3 expression and cl-Casp1 and cl-IL-1 β were prevented by aPC in all 3 cell types (Figure 3A-F). Thus, aPC dampens inflammasome activation not only in innate immune cells but also in resident cardiac cells. Although ATP is considered to induce inflammasome activation during myocardial IRI,³⁸ we ascertained the efficacy of aPC in the context of hypoxia reoxygenation (H/R) injury in cardiomyocytes. Exposure of primary neonatal cardiomyocytes to hypoxia (6 hours) followed by reoxygenation (12 hours) without prior LPS stimulation was sufficient for inflammasome activation, increased Nlrp3 expression, and cl-Casp1 and cl-IL-1 β (Figure 3G-H). H/R-induced inflammasome activation in primary cardiomyocytes was efficiently prevented by aPC (Figure 3G-H). Taken together, these findings show aPC prevents inflammasome activation both in innate immune cells (macrophages) and in resident cardiac cells (cardiomyocytes, cardiac fibroblasts).

aPC restricts inflammasome by suppressing mTORC1 and HK1

We next investigated the underlying mechanism by which aPC restricts Nlrp3 inflammasome activation. Cardioprotection by aPC after IRI has been linked with 5' adenosine monophosphate-activated protein kinase (AMPK) activation.²¹ Furthermore, mTOR complex 1 (mTORC1), which is negatively regulated by AMPK, was recently shown to activate Nlrp3 inflammasome in macrophages via hexokinase 1 (HK1).⁴⁰ Hence, we speculated that aPC restricts inflammasome activation by restricting mTORC1 signaling in the setting of myocardial IRI. To this end, we determined expression of Raptor (regulatory-associated protein of mTOR) and HK1 as well as total and phosphorylated ribosomal p70-S6 kinase (p70S6K) in BMDMs, neonatal cardiac fibroblasts, and neonatal cardiomyocytes. Expression of Raptor and HK1 and phosphorylation of p70S6K were enhanced in LPS-primed ATP-stimulated BMDMs and neonatal cardiac fibroblasts (Figure 4A-B; supplemental Figure 2A-B),⁴⁰ as well as in neonatal cardiomyocytes subjected to H/R (Figure 4C; supplemental Figure 2C). Treatment with aPC normalized expression of Raptor and HK1 and p70S6K phosphorylation levels in LPS-primed and ATP-stimulated cells or in H/R-injured primary cardiomyocytes (Figure 4A-C; supplemental Figure 2A-C). To corroborate the in vivo relevance of these findings, we analyzed heart tissue of mice with myocardial IRI. Treatment with aPC markedly reduced expression of Raptor and HK1 as well as phosphorylation of p70S6K in comparison with PBS-treated mice (control; Figure 4D-E). These data suggest that aPC restricts inflammasome activation by limiting mTORC1 activation.

To determine the mechanistic relevance of aPC-dependent mTORC1 regulation for inflammasome restriction, we used cells

lacking TSC1. TSC1 is a pivotal inhibitor of mTORC1, and its deficiency causes constitutive mTORC1 activation.⁴¹ BMDMs were isolated from mice with inducible TSC1 deficiency, and TSC1 expression was inhibited by transient expression with Cre recombinase *ex vivo*⁴¹ (Figure 4F; control cells transiently expressed GFP). In TSC1-deficient BMDMs, aPC failed to inhibit expression of Raptor and HK1 and phosphorylation of p70S6K (Figure 4G-H), and importantly, aPC-mediated Nlrp3 inflammasome restriction was abolished (Figure 4I-J). These results demonstrate that constitutive activation of mTORC1 signaling abolishes the inhibitory effect of aPC on inflammasome activation, establishing that aPC limits inflammasome activation by restricting mTORC1 activation.

aPC restricts inflammasome activation via PAR-1

To gain additional mechanistic insights and identify potential therapeutic targets, we ascertained the receptors involved. First, we analyzed expression of PARs and endothelial PC receptor (EPCR) in the different cell types employed in our study. Expression of PAR-1, PAR-2, PAR-3, PAR-4, and EPCR was readily detectable in these cells (supplemental Figure 3A). To determine the functional relevance of these receptors, we isolated BMDMs, neonatal cardiomyocytes, and cardiac fibroblasts from PAR-1^{-/-}, PAR-2^{-/-}, or PAR-3^{-/-} mice, and PAR-4 or EPCR function was blocked in wild-type cells using inhibitory antibodies.^{25,26} PAR-1 deficiency efficiently abolished Nlrp3 inflammasome suppression by aPC, whereas PAR-2 or PAR-3 deficiency and PAR-4 or EPCR blockage had no effect in any cell type studied (Figure 5A-C; supplemental Figure 3B-G). These *in vitro* results suggest that aPC restricts the inflammasome activation via PAR-1 in various cell types relevant for myocardial IRI.

To corroborate the *in vivo* relevance of the *in vitro* receptor studies, we employed the myocardial IRI model. Before myocardial IRI, mice were exposed to PBS (control), aPC alone, the aPC-HAPC1573 complex (the antibody HAPC1573 specifically blocks the anticoagulant function of aPC),^{24,27} or an aPC variant specifically lacking anticoagulant function (3K3A-aPC),^{28,29} or they were first treated with an inhibitory PAR-1 pepducin (P1pal-12S)^{26,30,31} followed by aPC treatment. Treatment with 3K3A-aPC or preincubation of aPC with the HAPC1573 antibody did not abolish the protective effect of aPC, as reflected by reduced infarct size (Figure 5D-F), reduced myocardial Nlrp3 expression and reduced cl-Casp1 and cl-IL-1 β (Figure 5G; supplemental Figure 4A), reduced myocardial caspase-1 activity (FLICA-Casp1 assay; Figure 5H; supplemental Figure 4B), and reduced plasma IL-1 β and IL-18 levels (Figure 5I-J). However, after inhibition of PAR-1, all these protective effects of aPC were lost (Figure 5D-J), verifying a pivotal function of PAR-1 in the cardioprotective effect of aPC in regard to myocardial IRI and inflammasome suppression.

Figure 5 (continued) (E-F) Treatment of mice with aPC-HAPC1573 complex or 3K3A-aPC reduces the infarct size as efficiently as aPC, and blocking PAR-1 signaling (pepducin P1pal-12S) abolishes the inhibitory effect of aPC. Representative heart sections showing infarcted area detected by triphenyl tetrazolium chloride staining (area encircled by dashed line; size bar, 20 μ m) (E) and dot plots summarizing data (F). (G-J) Treatment of mice with aPC-HAPC1573 complex or 3K3A-aPC reduces markers of inflammasome activation as efficiently as aPC, and blocking PAR-1 signaling (pepducin P1pal-12S) abolishes the inhibitory effect of aPC. (G) Representative immunoblots of cardiac Nlrp3 expression and cl-Casp1 and cl-IL-1 β , with GAPDH as loading control (cont); arrowheads indicate inactive (white) and active (black) forms of caspase-1 or IL-1 β . (H) Representative images of active caspase-1 within the infarcted tissue (frozen sections incubated with FLICA-Casp1 probes; size bar, 20 μ m). Dot plots summarizing plasma IL-1 β (I) and IL-18 (J) levels. Sham-operated (sham) or mice with myocardial IRI without (PBS; cont), with aPC (aPC), with aPC-HAPC1573 complex (aPC+HAPC1573), with an aPC variant specifically lacking anticoagulant function (3K3A-aPC), or with aPC and PAR-1 pepducin P1pal-12S (aPC+P1pal-12S) pretreatment. Data shown represent mean \pm SEM. Data obtained from at least 3 independent experiments each with at least 2 technical replicates (A-C) or from at least 6 mice per group (D-J). ***P* < .01; analysis of variance (F,I-J).

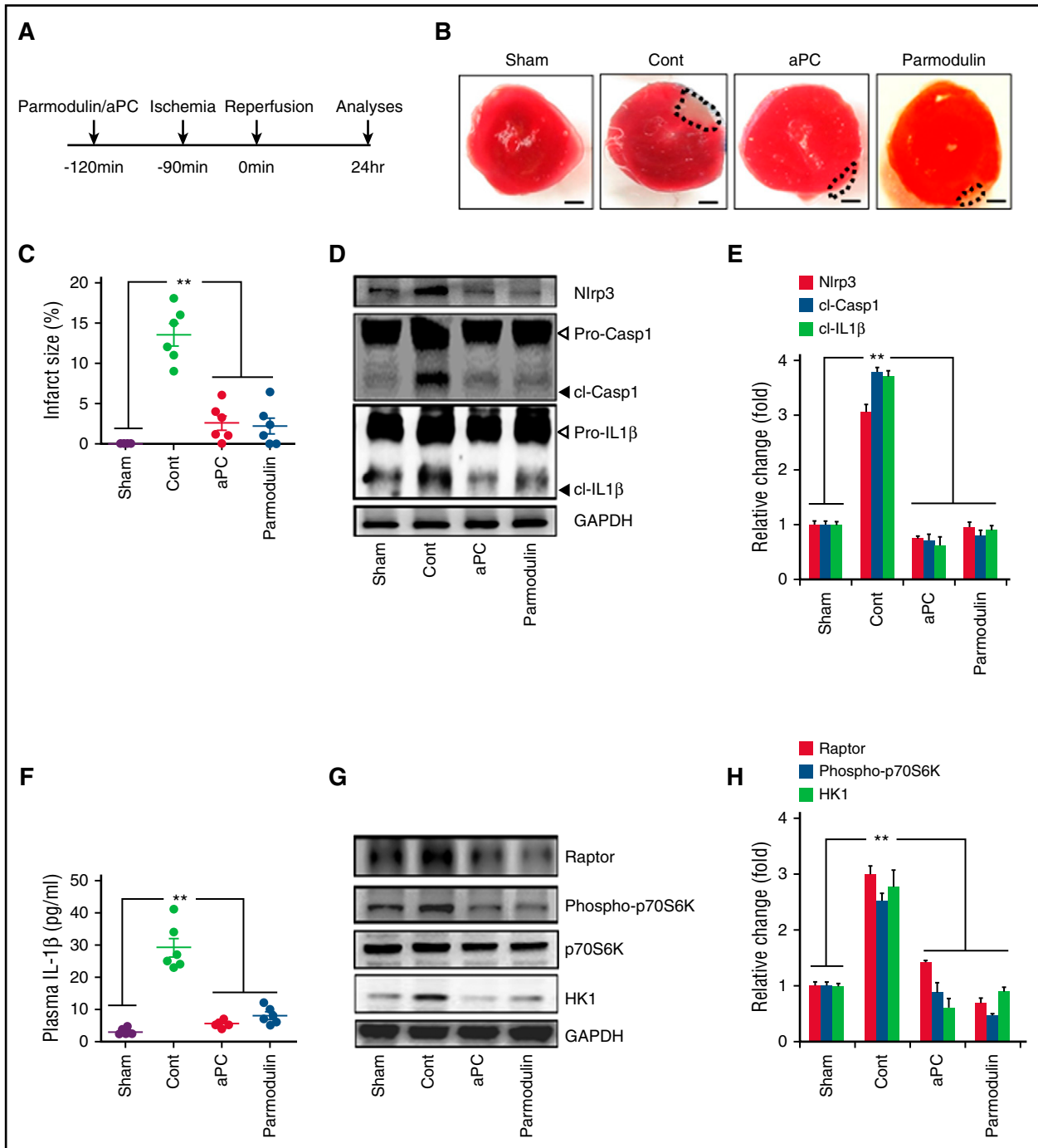


Figure 6. Par-1–specific parmodulin ameliorates inflammasome activation in myocardial IRI. (A) Experimental design. (B–C) The biased PAR-1 antagonist parmodulin-2 (5 mg/kg) reduces the infarcted area to the same extent as aPC. Representative heart sections showing infarcted area detected by TTC staining (infarcted area encircled by dashed line; size bar, 20 μ m) (B) and dot plot summarizing data (C). (D–H) Treatment of mice with parmodulin-2 reduces markers of inflammasome activation and mTORC1 signaling as efficiently as aPC. Representative immunoblots showing cardiac Nlrp3 expression and cl-Casp1 and cl-IL-1 β (D) and bar graph summarizing results, with glyceraldehyde-3-phosphate dehydrogenase (GAPDH) as loading control (cont) (E). (D) Arrowheads indicate inactive (white) and active (black) forms of caspase-1 or IL-1 β . (E) The active form was quantified. Dot plots summarizing plasma IL-1 β (F) and representative immunoblots showing Raptor and HK1 expression and total and phosphorylated p70S6K (G) and bar graph summarizing results, with GAPDH as loading control (H). Sham-operated mice (sham) or mice with myocardial IRI without (cont; PBS) or with aPC (aPC) or parmodulin-2 (parmodulin) pretreatment. Data shown represent mean \pm SEM of at least 6 mice per group (B–H). ** $P < .01$; analysis of variance (C,E–F,H).

PAR-1–specific parmodulin ameliorates inflammasome activation in myocardial IRI

Considering that aPC predominately requires PAR-1 for inflammasome restriction after myocardial IRI, we speculated that targeting

PAR-1 would be sufficient to mimic the effect of aPC. However, PAR-1 has pleiotropic effects and, depending on the activator and coreceptors involved, can convey via biased signaling cell-damaging or cell-protective effects.^{15,42} Recently, structural biochemistry–created compounds, parmodulins, were shown to block only specific aspects of

biased PAR signaling.³² We used parmodulin-2, which blocks cyto-disruptive, but not cytoprotective, PAR-1 signaling³² and evaluated its anti-inflammatory and cytoprotective effects in myocardial IRI. Treatment of mice with parmodulin-2 (5 mg/kg; Figure 6A) before myocardial IRI was as sufficient as that with aPC, reducing the infarct size (Figure 6B-C), cardiac expression of inflammasome regulators (Nlrp3, cl-Casp1, cl-IL1 β ; Figure 6D-E), and plasma IL-1 β levels (Figure 6F). Furthermore, parmodulin-2 efficiently reduced expression of Raptor and HK1 and phosphorylation of p70S6K (Figure 6G-H). Thus, mimicking biased aPC signaling via PAR-1 using parmodulins is sufficient to limit inflammasome activity and convey cardioprotection in myocardial IRI.

aPC protects against renal IRI by limiting Nlrp3 inflammasome activity

Considering recent data showing that inflammasome activation contributes to IRI in other tissues, including the kidney,^{43,44} we speculated that inflammasome suppression by aPC may have implications beyond myocardial IRI. To this end, we induced renal IRI following an established protocol.²⁵ Mice were pretreated with aPC (1 mg/kg bodyweight IP) or PBS 30 minutes before renal IRI (bilateral renal pedicle occlusion, 30 minutes). After 24 hours, we determined indices of renal failure and inflammasome activation (Figure 7A). As expected, BUN, creatinine, tubular injury, and expression of KIM-1 (kidney-injury-molecule 1) were induced in control mice as compared with sham-operated mice (Figure 7B-C; supplemental Figure 5A-C). Likewise, renal expression of Nlrp3 and cl-Casp1 and cl-IL-1 β as well as the presence of cl-Casp1 within renal medullary tubular cells were markedly reduced by aPC treatment (Figure 7D-G). In parallel, aPC treatment decreased plasma cytokines (IL-1 β , IL-18; Figure 7H-I). Importantly, Nlrp3 expression, which conveys renal injury at least in part independent of the canonical inflammasome (caspase-1, IL-1 β , IL-18), was not different in aPC-treated and sham-operated mice, suggesting that aPC treatment efficiently blocks canonical and noncanonical effects of Nlrp3. Congruent with results from myocardial IRI (Figure 2), aPC failed to reduce inflammasome activation or protect against renal IRI in Nlrp3^{V-ER} mice (Figure 7J-P; supplemental Figure 6A-C). Thus, as in the heart, renal inflammasome restriction by aPC depends on Nlrp3 suppression.

Discussion

Here we establish that aPC is an endogenous negative regulator of inflammasome activation after IRI, uncovering a new anti-inflammatory mechanism of aPC. We used 2 independent models, myocardial and renal IRIs, to demonstrate that aPC restricts Nlrp3 expression and activation of caspase-1 and IL-1 β . aPC treatment after onset of IRI efficiently restricts Nlrp3 inflammasome activation and is sufficient for cytoprotection, which is congruent with an improved outcome after inflammasome inhibition after myocardial IRI.⁴ In addition, we demonstrate that inflammasome restriction by aPC is independent of its anticoagulant properties but depends on signaling via PAR-1. Importantly, a biased agonist of PAR-1 (parmodulin-2) mimics inflammasome suppression and cytoprotection after myocardial IRI. Thus, we propose that biased agonists mimicking aPC signaling may be a new therapeutic approach in IRI.

Inflammasome activation after IRI occurs in various organs other than the heart and the kidney, including the brain and the liver.⁴⁵ In these organs, aPC likewise conveys cytoprotection after IRI,¹⁵

suggesting that limiting inflammasome activation by aPC may be relevant not only in the heart and kidney (as shown here), but also in other organs. Of note, the 3K3A aPC variant has pronounced neuroprotective effects in animal models of cerebral IRI and is undergoing clinical trials in patients experiencing stroke (registered at www.clinicaltrials.gov as #NCT02222714).⁴⁶ Because Nlrp3 inflammasome inhibition ameliorates experimental cerebral IRI, it is conceivable that aPC restricts Nlrp3 inflammasome activation in cerebral IRI, but this remains to be shown.

Nlrp3 overexpression itself is not sufficient to cause myocardial dysfunction³⁸ (as shown in the current study), corroborating that both the priming and activation steps are required for inflammasome activation after IRI.^{38,47} Importantly, by restricting Nlrp3 expression and caspase-1 and IL-1 β activation, aPC seems to target both inflammasome activation steps. Because the priming step of inflammasome activation is largely mediated by NF- κ B, and because aPC inhibits NF- κ B activity, the proposed function of aPC in restricting inflammasome priming is plausible.^{48,49} Considering the results obtained here using aPC and parmodulin-2 or recent studies using small-compound Nlrp3 inhibitors,⁵⁰ targeting both steps of Nlrp3 inflammasome seems to be therapeutically feasible. On the basis of these observations, we propose that simultaneously restricting the priming (induction of Nlrp3 expression) and activation (formation of the inflammasome complex) steps may be superior to inhibition of IL-1 receptor signaling or caspases.^{5,51,52}

Both canonical (IL-1 β , IL-18) and noncanonical (Nlrp3 or caspase-1) inflammasome-dependent effects cause tissue damage after IRI.^{6-8,53} Thus, in myocardial fibroblasts, Nlrp3 induces mitochondrial ROS and Smad signaling directly through its NACHT domain.⁵³ Likewise, in renal IRI, Nlrp3 conveys tissue damage independent of ASC and cytokine production.⁵⁴ Whether aPC regulates the canonical Nlrp3 activation pathway, the noncanonical Nlrp3 activation via caspase-11, or both needs to be further evaluated in future studies.

The current results suggest that inflammasome activation and associated cell death (pyroptosis) are mechanistically more relevant than apoptosis in IRI. A role of apoptosis, an immunologically silent cell-death form, in myocardial IRI has been repeatedly proposed, but these studies have typically used terminal deoxynucleotidyltransferase-mediated dUTP nick end labeling assay, which is not specific for apoptosis and additionally detects pyroptosis and other cell-death forms.^{4,5,17,19} Our in vivo kinetic studies demonstrate that inflammasome activation precedes apoptosis (Figure 2). Additionally, Nlrp3 deficiency is protective in myocardial IRI.⁶ Inflammasome activation and pyroptosis in tissue-resident cells after IRI may generate a proinflammatory microenvironment leading to the recruitment of professional immune cells. This may trigger a vicious cycle promoting tissue damage.^{47,55,56} Targeting the Nlrp3 inflammasome or caspase-1 may inhibit very early tissue-disruptive events and thus may be superior to other approaches limiting inflammation associated with IRI. However, the current study does not exclude the occurrence or relevance of apoptosis in IRI. Indeed, the induction of apoptosis at later stages after IRI may reflect a protective mechanism, eliminating damaged cells without simultaneously inducing an inflammatory response.

What might be the mechanisms underlying aPC-mediated inflammasome inhibition? Here we show that inflammasome inhibition by aPC depends on mTORC1 inhibition. mTORC1 activation and induction of HK1 expression and glycolysis constitute a mechanism of Nlrp3, but not of Nlrp1 or Nlrp4, activation in macrophages.⁵⁷ Likewise, we observed inhibition of mTORC1 and HK1 in LPS- and ATP-challenged macrophages and cardiac fibroblasts by aPC. In addition, aPC inhibited mTORC1 and HK1 in hypoxia/reoxygenation-challenged cardiomyocytes as well as in the heart

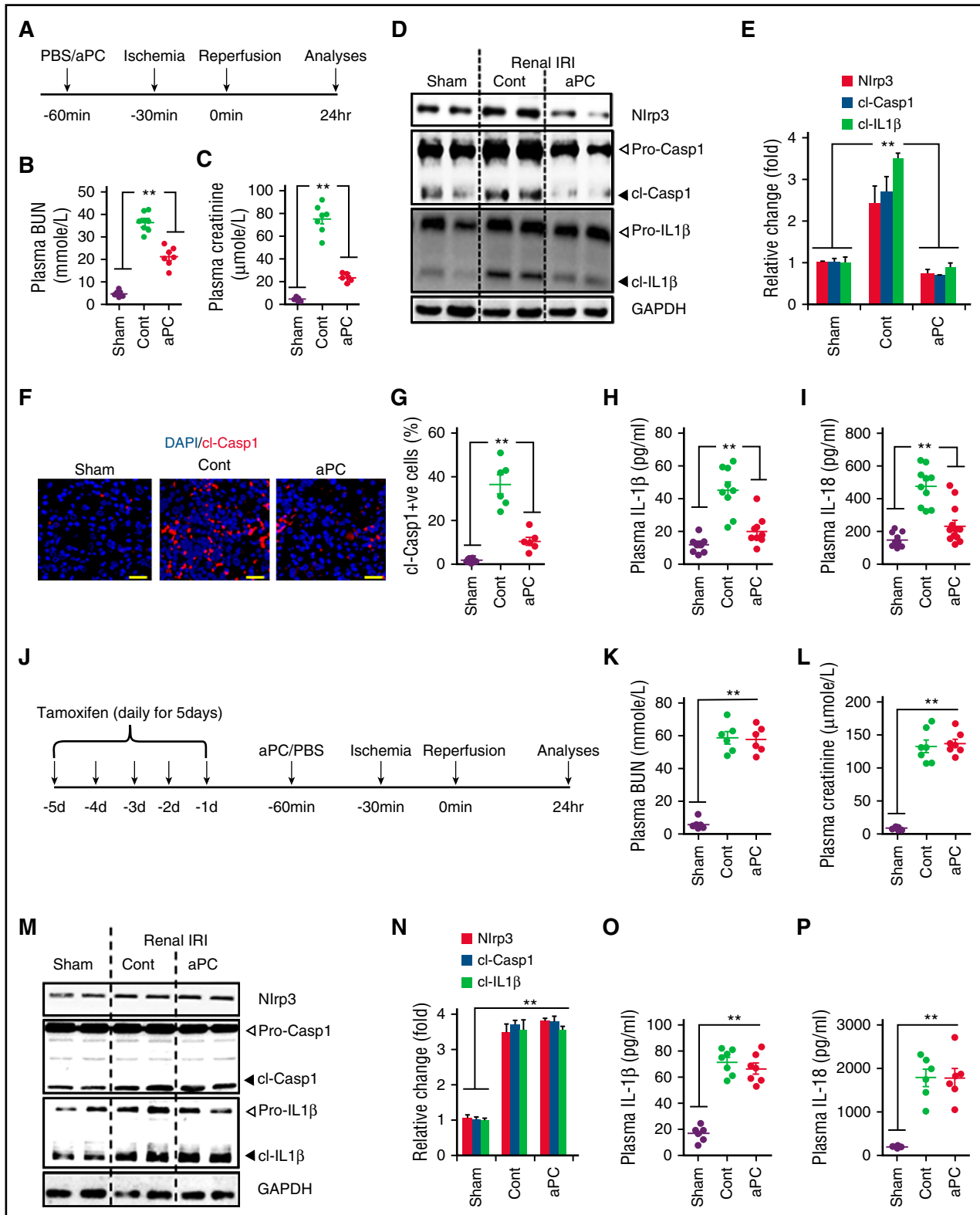


Figure 7. aPC restricts Nlrp3 inflammasome activation in renal IRI. (A) Experimental design. aPC treatment reduces plasma BUN (B) and creatinine (C) levels in mice with bilateral renal pedicle occlusion (30 minutes) and reperfusion for 24 hours. (D-I) aPC reduces renal IRI-induced inflammasome activation. Representative immunoblots of renal Nlrp3 expression and cl-Casp1 and cl-IL-1β (D) and bar graph summarizing results, with glyceraldehyde-3-phosphate dehydrogenase (GAPDH) as loading control (cont) (E). (D) Arrowheads indicate inactive (white) and active (black) forms of caspase-1 or IL-1β. (E) The active form was quantified. Representative images of active caspase-1 within renal medullary tubular cells (frozen sections antibody specific for cl-Casp1; size bar, 20 μm) (F) and dot plot summarizing data (G). Dot plots summarizing plasma IL-1β (H) and IL-18 levels (I). (J) Experimental design. (K-P) aPC fails to reduce Nlrp3 expression, cl-Casp1 or cl-IL-1β, or plasma IL-1β or IL-18 levels in Nlrp3^{V-ER} mice after renal IRI. Plasma BUN (K) and creatinine (L) levels (dot plots); representative immunoblots of renal Nlrp3 expression and cl-Casp1 and cl-IL-1β (M) and bar graph summarizing results (N). Arrowheads indicate inactive (white) and active (black) forms of caspase-1 or IL-1β (M); only the active form was quantified (N); GAPDH as loading control; dot plots of plasma IL-1β and IL-18 levels (O-P). Sham-operated mice (sham) or mice with renal IRI without (cont; PBS) or with aPC pretreatment (aPC) treatment. Data shown represent mean ± SEM of at least 6 different mice per group (B-I, K-P). **P < .01; analysis of variance (B-C, E, G-I, K-L, N-P).

after myocardial IRI. Inhibition of mTORC1 by aPC is congruent with AMPK activation (an inhibitor of mTORC1 signaling) by aPC after myocardial infarction.²¹ mTORC1 activation in IRI has frequently been observed,^{58,59} corroborating a mechanistic relevance of mTORC1 inhibition by aPC. We acknowledge that the role of mTOR signaling in myocardial IRI is complex and depends on its temporal activation pattern, the cell type, the extent of mTOR activity, and the involvement of mTORC1 vs mTORC2.^{14,41,60} The ability of TSC1 deficiency to abolish aPC-mediated mTORC1 inhibition indicates that aPC regulates the mTORC1 complex.^{60,61} However, considering the multifaceted interactions of TSC1/TSC2, mTORC1, and mTORC2, the precise mechanism needs to be evaluated in future studies.

We and others have demonstrated that aPC restricts mitochondrial ROS,^{24,62} a known inducer of Nlrp3 inflammasome activation.⁴⁵ Intriguingly, mTORC1 regulates mitochondrial quality and ROS,⁶³ suggesting that inhibition of mTORC1 and mitochondrial ROS by aPC may be mechanistically linked. Because the regulation of mitochondrial ROS and mTORC1 is mutual,⁶⁴ additional studies are required to decipher the exact mechanism through which aPC regulates mTORC1 and mitochondrial ROS.

Although it provides new insights into the cytoprotective effects of aPC, the current study also raises questions. Thus, although parmodulin-2 demonstrated efficacy in the study, it currently remains unknown whether mimicking biased signaling via PAR-1 is sufficient to copy the versatile cytoprotective effects of aPC. Considering that parmodulin-2 targets Gαq signaling, we suspect that aPC–PAR-1–Gαq signaling conveys aPC-mediated inflammasome suppression.³² Furthermore, various receptors complement aPC signaling via PAR-1 in cell- and context-specific fashions.^{26,65,66} The coreceptors required for aPC PAR-1-mediated inflammasome suppression remain unknown. Deciphering the specific coreceptors and signaling pathways involved may allow further optimization of a molecular targeted therapy to inhibit inflammasome activation after IRI.

Additionally, the long-term outcome after interventions with aPC in the setting of myocardial IRI remains to be evaluated. Several groups have shown that inflammasome inhibition improves cardiac remodeling and function at later time points.^{4,5,67} Because aPC ameliorates angiotensin II-triggered myocardial remodeling,²² an improved outcome after aPC-mediated inflammasome restriction seems conceivable, but this remains to be shown.

We demonstrate inflammasome suppression by aPC in various cell types relevant in myocardial IRI. Whether inflammasome suppression in a particular cell type is more important than in others in the context of IRI remains to be shown. Intriguingly, the proposed initiation of a vicious cycle by inflammasome activation in tissue-resident cells, which then promotes the recruitment and activation of inflammatory cells, implies that it may be sufficient to inhibit inflammasome

activation specifically in ischemic organs. This may allow tissue protection without compromising the function of innate immune cells, which may constitute an advantage in organ transplantation or in patients in an intensive care unit setting.

Acknowledgments

The authors thank Johannes Lauf, Kathrin Deneser, Julia Judin, Juliane Friedrich, René Rudat, Rumiya Makarova, Xiao Xu, and Jose A. Fernandez for excellent technical support.

This work was supported by grants IS-67/5-3, IS-67/8-1, IS-67/11-1, and CRC854/B26 (B.I.), SH 849/1-2 (K.S.), and CRC1140, CRC 992, and HU 1016/8-1 (T.B.H.) from the Deutsche Forschungsgemeinschaft; the Stiftung Pathobiochemie und Molekulare Diagnostik (K.S.); grants UMI-HL120877 (C.T.E.) and HL052246 (J.H.G.) from the National Institutes of Health (NIH), National Heart, Lung, and Blood Institute; grant 01GM1518C from the German Federal Ministry of Education and Research (T.B.H.); grant 616891 from the European Research Council (T.B.H.); the Biomarker Enterprise to Attack Diabetic Kidney Disease, Horizon 2020 Innovative Medicine Initiative 2 Consortium (T.B.H.); grant 1R15HL127636 from the NIH, National Heart, Lung, and Blood Institute (C.D.); and German Academic Exchange Service scholarships (M.M.A.-D., A.E.).

Authorship

Contribution: S.N. performed and interpreted experiments; I.G. performed histological analyses; M.M.A.-D., S.K., A.E., and S.R. performed mouse experiments; S.G., J.M., and F.B. assisted in primary cell isolation work; T.B.H., C.D., E.C., C.T.E., and J.H.G. provided reagents and assisted in manuscript preparation; R.C.B.-D. assisted in manuscript preparation; and K.S. and B.I. conceptually designed and interpreted the experimental work and prepared the manuscript.

Conflict-of-interest disclosure: C.D. is an inventor on a patent (WO2012/040636) describing parmodulin-2 (ML161). The remaining authors declare no competing financial interests.

Correspondence: Khurram Shahzad, Department of Clinical Chemistry and Pathobiochemistry, Otto-von-Guericke-University Magdeburg, Leipziger Str 44, 39120 Magdeburg, Germany; e-mail: khurram.shahzad@med.ovgu.de; and Berend Isermann, Department of Clinical Chemistry and Pathobiochemistry, Otto-von-Guericke-University Magdeburg, Leipziger Str 44, 39120 Magdeburg, Germany; e-mail: berend.isermann@med.ovgu.de.

References

- Arslan F, de Kleijn DP, Pasterkamp G. Innate immune signaling in cardiac ischemia. *Nat Rev Cardiol*. 2011;8(5):292-300.
- Timmers L, Pasterkamp G, de Hoog VC, Arslan F, Appelman Y, de Kleijn DP. The innate immune response in reperfused myocardium. *Cardiovasc Res*. 2012;94(2):276-283.
- Marchant DJ, Boyd JH, Lin DC, Granville DJ, Garmaroudi FS, McManus BM. Inflammation in myocardial diseases. *Circ Res*. 2012;110(1):126-144.
- Abbate A, Salloum FN, Vecile E, et al. Anakinra, a recombinant human interleukin-1 receptor antagonist, inhibits apoptosis in experimental acute myocardial infarction. *Circulation*. 2008;117(20):2670-2683.
- Salloum FN, Chau V, Varma A, et al. Anakinra in experimental acute myocardial infarction—does dosage or duration of treatment matter? *Cardiovasc Drugs Ther*. 2009;23(2):129-135.
- Sandanger Ø, Ranheim T, Vinge LE, et al. The NLRP3 inflammasome is up-regulated in cardiac fibroblasts and mediates myocardial ischaemia-reperfusion injury. *Cardiovasc Res*. 2013;99(1):164-174.
- Kawaguchi M, Takahashi M, Hata T, et al. Inflammasome activation of cardiac fibroblasts is essential for myocardial ischemia/reperfusion injury. *Circulation*. 2011;123(6):594-604.
- Mezzaroma E, Toldo S, Farkas D, et al. The inflammasome promotes adverse cardiac remodeling following acute myocardial infarction in the mouse. *Proc Natl Acad Sci USA*. 2011;108(49):19725-19730.
- Guo H, Callaway JB, Ting JP. Inflammasomes: mechanism of action, role in disease, and therapeutics. *Nat Med*. 2015;21(7):677-687.
- Patti G, D'Ambrosio A, Mega S, et al. Early interleukin-1 receptor antagonist elevation in patients with acute myocardial infarction. *J Am Coll Cardiol*. 2004;43(1):35-38.
- Airaghi L, Lettino M, Manfredi MG, Lipton JM, Catania A. Endogenous cytokine antagonists

- during myocardial ischemia and thrombolytic therapy. *Am Heart J*. 1995;130(2):204-211.
12. Dinarello CA. Interleukin-1. *Cytokine Growth Factor Rev*. 1997;8(4):253-265.
 13. Borissoff JI, Spronk HM, ten Cate H. The hemostatic system as a modulator of atherosclerosis. *N Engl J Med*. 2011;364(18):1746-1760.
 14. Völkers M, Konstandin MH, Doroudgar S, et al. Mechanistic target of rapamycin complex 2 protects the heart from ischemic damage. *Circulation*. 2013;128(19):2132-2144.
 15. Griffin JH, Zlokovic BV, Mosnier LO. Activated protein C: biased for translation. *Blood*. 2015;125(19):2898-2907.
 16. Martí-Carvajal AJ, Solà I, Lathyris D, Cardona AF. Human recombinant activated protein C for severe sepsis. *Cochrane Database Syst Rev*. 2012;3:CD004388.
 17. Pirat B, Muderrisoglu H, Unal MT, et al. Recombinant human-activated protein C inhibits cardiomyocyte apoptosis in a rat model of myocardial ischemia-reperfusion. *Coron Artery Dis*. 2007;18(1):61-66.
 18. Maehata Y, Miyagawa S, Sawa Y. Activated protein C has a protective effect against myocardial I/R injury by improvement of endothelial function and activation of AKT1. *PLoS One*. 2012;7(8):e38738.
 19. Loubele ST, Spek CA, Leenders P, et al. Activated protein C protects against myocardial ischemia/reperfusion injury via inhibition of apoptosis and inflammation. *Arterioscler Thromb Vasc Biol*. 2009;29(7):1087-1092.
 20. Ding JW, Tong XH, Yang J, et al. Activated protein C protects myocardium via activation of anti-apoptotic pathways of survival in ischemia-reperfused rat heart. *J Korean Med Sci*. 2010;25(11):1609-1615.
 21. Wang J, Yang L, Rezaie AR, Li J. Activated protein C protects against myocardial ischemic/reperfusion injury through AMP-activated protein kinase signaling. *J Thromb Haemost*. 2011;9(7):1308-1317.
 22. Sopel MJ, Rosin NL, Falkenham AG, et al. Treatment with activated protein C (aPC) is protective during the development of myocardial fibrosis: an angiotensin II infusion model in mice. *PLoS One*. 2012;7(9):e45663.
 23. Vince JE, Silke J. The intersection of cell death and inflammasome activation. *Cell Mol Life Sci*. 2016;73(11-12):2349-2367.
 24. Bock F, Shahzad K, Wang H, et al. Activated protein C ameliorates diabetic nephropathy by epigenetically inhibiting the redox enzyme p66Shc. *Proc Natl Acad Sci USA*. 2013;110(2):648-653.
 25. Dong W, Wang H, Shahzad K, et al. Activated protein C ameliorates renal ischemia-reperfusion injury by restricting Y-box binding protein-1 ubiquitination. *J Am Soc Nephrol*. 2015;26(11):2789-2799.
 26. Madhusudhan T, Wang H, Straub BK, et al. Cytoprotective signaling by activated protein C requires protease-activated receptor-3 in podocytes. *Blood*. 2012;119(3):874-883.
 27. Xu J, Ji Y, Zhang X, Drake M, Esmon CT. Endogenous activated protein C signaling is critical to protection of mice from lipopolysaccharide-induced septic shock. *J Thromb Haemost*. 2009;7(5):851-856.
 28. Mosnier LO, Gale AJ, Yegneswaran S, Griffin JH. Activated protein C variants with normal cytoprotective but reduced anticoagulant activity. *Blood*. 2004;104(6):1740-1744.
 29. Wang Y, Zhao Z, Chow N, et al. Activated protein C analog protects from ischemic stroke and extends the therapeutic window of tissue-type plasminogen activator in aged female mice and hypertensive rats. *Stroke*. 2013;44(12):3529-3536.
 30. Kaneider NC, Leger AJ, Agarwal A, et al. 'Role reversal' for the receptor PAR1 in sepsis-induced vascular damage. *Nat Immunol*. 2007;8(12):1303-1312.
 31. Seehaus S, Shahzad K, Kashif M, et al. Hypercoagulability inhibits monocyte transendothelial migration through protease-activated receptor-1-, phospholipase-Cbeta-, phosphoinositide 3-kinase-, and nitric oxide-dependent signaling in monocytes and promotes plaque stability. *Circulation*. 2009;120(9):774-784.
 32. Aisiku O, Peters CG, De Ceunynck K, et al. Parmodulins inhibit thrombus formation without inducing endothelial injury caused by vorapaxar. *Blood*. 2015;125(12):1976-1985.
 33. Dockendorff C, Aisiku O, Verplank L, et al. Discovery of 1,3-diaminobenzenes as selective inhibitors of platelet activation at the PAR1 receptor. *ACS Med Chem Lett*. 2012;3(3):232-237.
 34. Shahzad K, Bock F, Al-Dabet MM, et al. Caspase-1, but not caspase-3, promotes diabetic nephropathy. *J Am Soc Nephrol*. 2016;27(8):2270-2275.
 35. Weischenfeldt J, Porse B. Bone marrow-derived macrophages (BMM): isolation and applications. *CSH Protoc*. 2008;2008.pdb.prot5080.
 36. Finsen AV, Lunde IG, Sjaastad I, et al. Syndecan-4 is essential for development of concentric myocardial hypertrophy via stretch-induced activation of the calcineurin-NFAT pathway. *PLoS One*. 2011;6(12):e28302.
 37. Kain V, Prabhu SD, Halade GV. Inflammation revisited: inflammation versus resolution of inflammation following myocardial infarction. *Basic Res Cardiol*. 2014;109(6):444.
 38. Toldo S, Mezzaroma E, McGeough MD, et al. Independent roles of the priming and the triggering of the NLRP3 inflammasome in the heart. *Cardiovasc Res*. 2015;105(2):203-212.
 39. Xie M, Yu Y, Kang R, et al. PKM2-dependent glycolysis promotes NLRP3 and AIM2 inflammasome activation. *Nat Commun*. 2016;7:13280.
 40. Moon JS, Hisata S, Park MA, et al. mTORC1-induced HK1-dependent glycolysis regulates NLRP3 inflammasome activation. *Cell Reports*. 2015;12(1):102-115.
 41. Howell JJ, Hellberg K, Turner M, et al. Metformin inhibits hepatic mTORC1 signaling via dose-dependent mechanisms involving AMPK and the TSC complex. *Cell Metab*. 2017;25(2):463-471.
 42. Mosnier LO, Sinha RK, Burnier L, Bouwens EA, Griffin JH. Biased agonism of protease-activated receptor 1 by activated protein C caused by noncanonical cleavage at Arg46. *Blood*. 2012;120(26):5237-5246.
 43. Kim HJ, Lee DW, Ravichandran K, et al. NLRP3 inflammasome knockout mice are protected against ischemic but not cisplatin-induced acute kidney injury. *J Pharmacol Exp Ther*. 2013;346(3):465-472.
 44. Szeto HH, Liu S, Soong Y, et al. Mitochondria protection after acute ischemia prevents prolonged upregulation of IL-1 β and IL-18 and arrests CKD. *J Am Soc Nephrol*. 2017;28(5):1437-1449.
 45. Minutoli L, Puzzolo D, Rinaldi M, et al. ROS-mediated NLRP3 inflammasome activation in brain, heart, kidney, and testis ischemia/reperfusion injury. *Oxid Med Cell Longev*. 2016;2016:2183026.
 46. Lyden P, Levy H, Weymer S, et al. Phase 1 safety, tolerability and pharmacokinetics of 3K3A-APC in healthy adult volunteers. *Curr Pharm Des*. 2013;19(42):7479-7485.
 47. Takahashi M. NLRP3 inflammasome as a novel player in myocardial infarction. *Int Heart J*. 2014;55(2):101-105.
 48. Joyce DE, Gelbert L, Ciaccia A, DeHoff B, Grinnell BW. Gene expression profile of antithrombotic protein c defines new mechanisms modulating inflammation and apoptosis. *J Biol Chem*. 2001;276(14):11199-11203.
 49. Latz E, Xiao TS, Stutz A. Activation and regulation of the inflammasomes. *Nat Rev Immunol*. 2013;13(6):397-411.
 50. van Hout GP, Bosch L, Ellenbroek GH, et al. The selective NLRP3-inflammasome inhibitor MCC950 reduces infarct size and preserves cardiac function in a pig model of myocardial infarction. *Eur Heart J*. 2017;38(11):828-836.
 51. Kovacs P, Bak I, Szendrei L, et al. Non-specific caspase inhibition reduces infarct size and improves post-ischaemic recovery in isolated ischaemic/reperfused rat hearts. *Naunyn Schmiedebergs Arch Pharmacol*. 2001;364(6):501-507.
 52. Mocanu MM, Baxter GF, Yellon DM. Caspase inhibition and limitation of myocardial infarct size: protection against lethal reperfusion injury. *Br J Pharmacol*. 2000;130(2):197-200.
 53. Bracey NA, Gershkovich B, Chun J, et al. Mitochondrial NLRP3 protein induces reactive oxygen species to promote Smad protein signaling and fibrosis independent from the inflammasome. *J Biol Chem*. 2014;289(28):19571-19584.
 54. Shigeoka AA, Mueller JL, Kambo A, et al. An inflammasome-independent role for epithelial-expressed Nlrp3 in renal ischemia-reperfusion injury. *J Immunol*. 2010;185(10):6277-6285.
 55. Ikeda U, Ikeda M, Kano S, Shimada K. Neutrophil adherence to rat cardiac myocyte by proinflammatory cytokines. *J Cardiovasc Pharmacol*. 1994;23(4):647-652.
 56. Grundmann S, Bode C, Moser M. Inflammasome activation in reperfusion injury: friendly fire on myocardial infarction? *Circulation*. 2011;123(6):574-576.
 57. Moon JS, Nakahira K, Chung KP, et al. NOX4-dependent fatty acid oxidation promotes NLRP3 inflammasome activation in macrophages. *Nat Med*. 2016;22(9):1002-1012.
 58. Kezic A, Becker JU, Thaiss F. The effect of mTOR-inhibition on NF- κ B activity in kidney ischemia-reperfusion injury in mice. *Transplant Proc*. 2013;45(5):1708-1714.
 59. Huang L, Dai K, Chen M, et al. The AMPK agonist PT1 and mTOR inhibitor 3HOI-BA-01 protect cardiomyocytes after ischemia through induction of autophagy. *J Cardiovasc Pharmacol Ther*. 2016;21(1):70-81.
 60. Saxton RA, Sabatini DM. mTOR signaling in growth, metabolism, and disease. *Cell*. 2017;168(6):960-976.
 61. Dalle Pezze P, Sonntag AG, Thien A, et al. A dynamic network model of mTOR signaling reveals TSC-independent mTORC2 regulation. *Sci Signal*. 2012;5(217):ra25.
 62. Yamaji K, Wang Y, Liu Y, et al. Activated protein C, a natural anticoagulant protein, has antioxidant properties and inhibits lipid peroxidation and advanced glycation end products formation. *Thromb Res*. 2005;115(4):319-325.

63. Baltzer C, Tiefenböck SK, Frei C. Mitochondria in response to nutrients and nutrient-sensitive pathways. *Mitochondrion*. 2010;10(6):589-597.
64. Darzynkiewicz Z, Zhao H, Halicka HD, et al. In search of antiaging modalities: evaluation of mTOR- and ROS/DNA damage-signaling by cytometry. *Cytometry A*. 2014;85(5):386-399.
65. Weiler H. Multiple receptor-mediated functions of activated protein C. *Hämostaseologie*. 2011;31(3):185-195.
66. Burnier L, Mosnier LO. Novel mechanisms for activated protein C cytoprotective activities involving noncanonical activation of protease-activated receptor 3. *Blood*. 2013;122(5):807-816.
67. Butts B, Gary RA, Dunbar SB, Butler J. The importance of NLRP3 inflammasome in heart failure. *J Card Fail*. 2015;21(7):586-593.



blood[®]

2017 130: 2664-2677

doi:10.1182/blood-2017-05-782102 originally published
online September 7, 2017

Cytoprotective activated protein C averts Nlrp3 inflammasome–induced ischemia-reperfusion injury via mTORC1 inhibition

Sumra Nazir, Ihsan Gadi, Moh'd Mohanad Al-Dabet, Ahmed Elwakiel, Shrey Kohli, Sanchita Ghosh, Jayakumar Manoharan, Satish Ranjan, Fabian Bock, Ruediger C. Braun-Düllaeus, Charles T. Esmon, Tobias B. Huber, Eric Camerer, Chris Dockendorff, John H. Griffin, Berend Isermann and Khurram Shahzad

Updated information and services can be found at:

<http://www.bloodjournal.org/content/130/24/2664.full.html>

Articles on similar topics can be found in the following Blood collections

[Thrombosis and Hemostasis](#) (1125 articles)

Information about reproducing this article in parts or in its entirety may be found online at:

http://www.bloodjournal.org/site/misc/rights.xhtml#repub_requests

Information about ordering reprints may be found online at:

<http://www.bloodjournal.org/site/misc/rights.xhtml#reprints>

Information about subscriptions and ASH membership may be found online at:

<http://www.bloodjournal.org/site/subscriptions/index.xhtml>